CHAPTER 7

Processing, Tensile Testing and Thermal Properties of PLC Monofilament Fibres

7.1 Introduction

In this Chapter, attention is focused especially on the monofilament fibre processing of the PLC copolymers by melt spinning and on the improvement of their mechanical properties for use as absorbable surgical sutures.

Fibres used in relation to health care and surgery may be classified as biodegradable or non-degradable. All fibres used for this application must be nontoxic, non-allergenic, and non-carcinogenic and must also be able to be sterilized without imparting any changes in their physical or chemical characteristics.

In our research, PLC was prepared to use as biodegradable absorbable monofilament suture with a composition of LL:CL = 75:25 mol %. L-lactide (LL) and ε-caprolactone (CL) are biodegradable and biocompatible in the human body and so are widely used as components for surgery such as absorbable surgical sutures (see Table 1.1). LL is the main component to give high crystallinity and lower cost while CL increases chain flexibility and lowers fibre stiffness. The PLC copolymers were synthesised via bulk ring-opening polymerisation using various novel tin(II) alkoxides as described in Chapter 6.

7.2 Melt Spinning

The melt spinning process was used to fabricate monofilament fibres in this research because it introduces fewer impurities than other solvent-based processes such as wet spinning. Figure 7.1 shows a photograph of the small-scale melt spinning apparatus used in this work which could handle batch sizes of as small as 20 g.

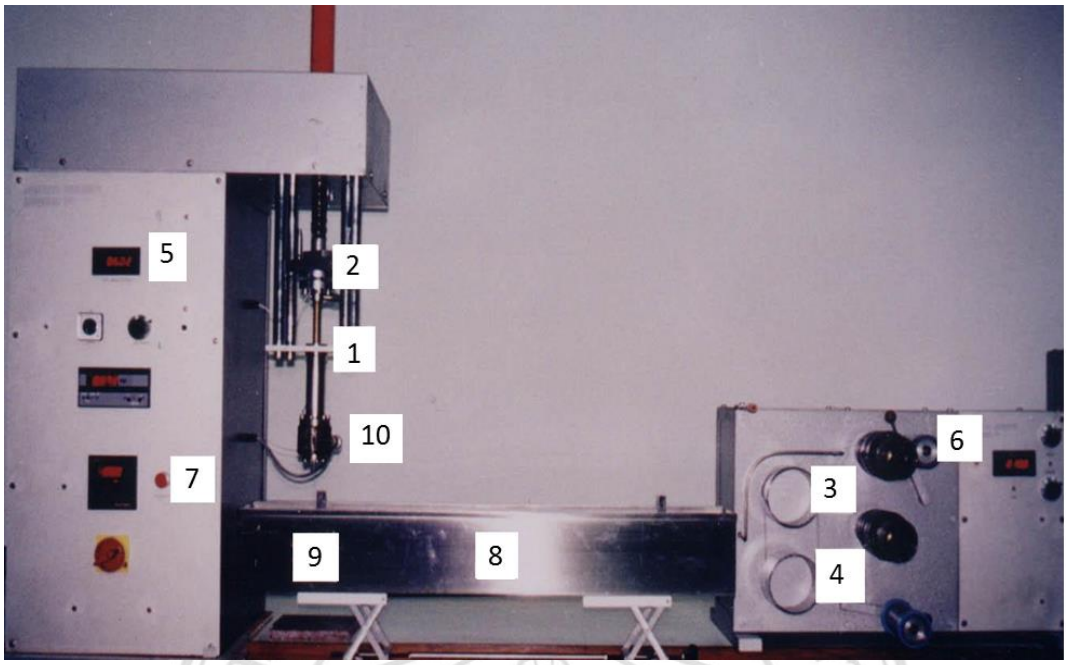

Figure 7.1 Small-scale melt spinning apparatus

1 = extrusion cylinder
2 = piston (ram) in raised position
3 = godet
4 = godet
5 = ram speed indicator (mm/min)
6 = final take-up bobbin
7 = heater control switch
8 = cooling bath (ice-water)
9 = filament guide
10 = heating block\

Prior to melt spinning, the PLC samples were first compressed into pre-formed cylindrical rods. Melt spinning from rods gave fibre of more consistent quality than from beads or small pieces and also reduced the tendency for void formation. A closer view of the various accessories used is shown in the photographs in Figures 7.2 and 7.3.

Each PLC copolymer, which had previously been dried in a vacuum oven at 55^0C, was placed in the pre-forming cylinder. The cylinder assembly was placed in the extrusion unit of the melt spinning apparatus shown in Figure 7.1, the heater plug connected and the thermocouple inserted into its hole. The copolymer pieces were then compressed at a suitable temperature just below T_m (from DSC) so that they softened (partially melted) just enough to stick together in the shape of a cylindrical rod [99]. Ideally, the surface of the rod was smooth with the outline of the pieces still visible where they were fused together.

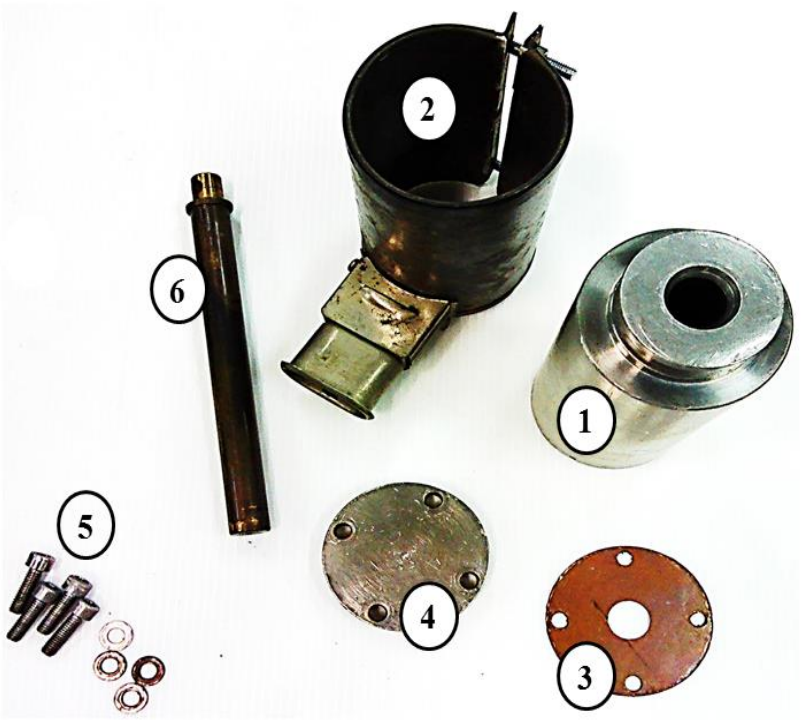

Figure 7.2 The various melt spinning apparatus accessories used in the preparation of PLC rods: 1. Pre-forming cylinder, 2. Heater band, 3. Copper gasket, 4. Plain blanking plate, 5. Cap screws and 6. Piston (ram).

Figure 7.3 The assembled cylinder used for making a copolymer rod.

Following the pre-formed rod preparation, the various accessories used in melt spinning (Figure 7.4) were assembled as shown in Figure 7.5 and the extrusion cylinder

complete with band heater placed in the extrusion unit of the melt spinning apparatus in Figure 7.1.

A pre-formed PLC rod was then heated up to the required melt spinning temperature and, when the temperature had reached equilibrium, the ram was lowered at the chosen speed to compress and extrude the molten PLC through a plate containing a small single hole of 1.00 mm diameter, called a spinnerette. Before reaching the spinnerette, the molten copolymer passed through a stainless steel filter mesh. Filtration is needed in order to separate any non-melted impurities which might otherwise accidentally contaminate the polymer and later on cause discontinuities in the filament or even plug the spinnerette hole. It is also claimed that passing through the mesh shears the melt and, in doing so, improves the melt rheology. The extruded filament was then fast-cooled (quenched) by passing through the ice-water cooling bath (2-5 ^{o}C) before being wound around take-up rollers and collected on a bobbin (Figure 7.6).

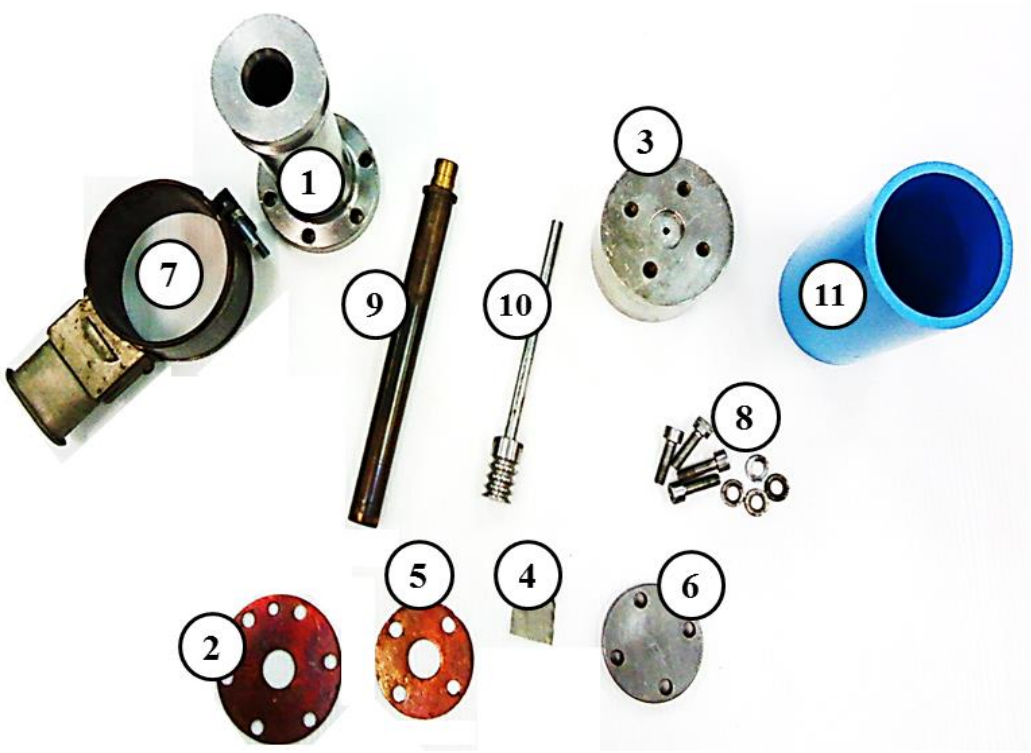

Figure 7.4 The various accessories used in the melt spinning of the pre-forming PLC rods: 1. Extrusion cylinder, 2. Gasket used between the extrusion cylinder and the heater block, 3. Heating block, 4. Stainless steel filter mesh, 5. Gasket used between the heater block and the spinetette, 6 Spinnerette, 7. Heater band, 8.Cap screws, 9. Piston, 10. Filament guide and 11. Filament spool.

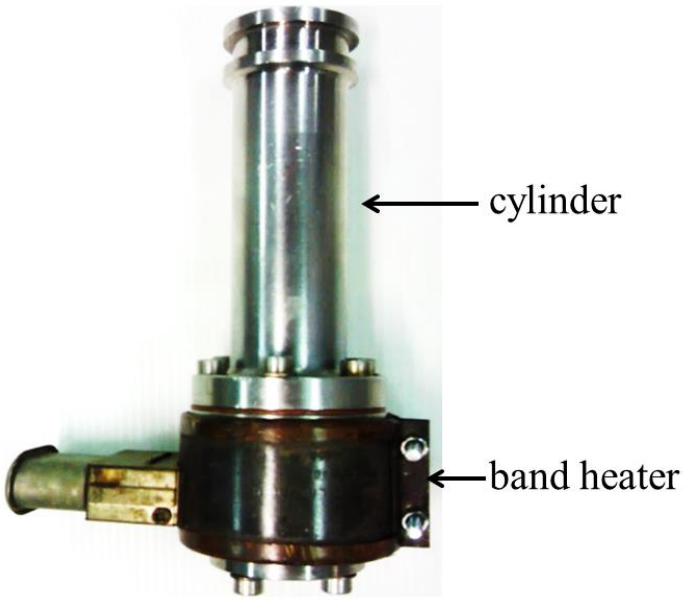

Figure 7.5 The assembled cylinder used for fibre processing.

In order to be able to obtain as-spun fibres with limited crystallinity and little or no molecular orientation, low spinning speeds with minimal draw were employed with the emphasis on producing fibres of uniform diameter. The ram (piston) speed used was 2.0 mm/min which, when combined with the cylinder diameter of 15 mm and the spinnerette diameter of 1 mm, corresponded to a fibre extrusion rate of 45 cm/min. The as-spun fibre's mechanical properties could then be improved by a succession of controlled off-line drawing and annealing steps. The PLC rods and as-spun fibres obtained are shown in Tables 7.1 and 7.2.

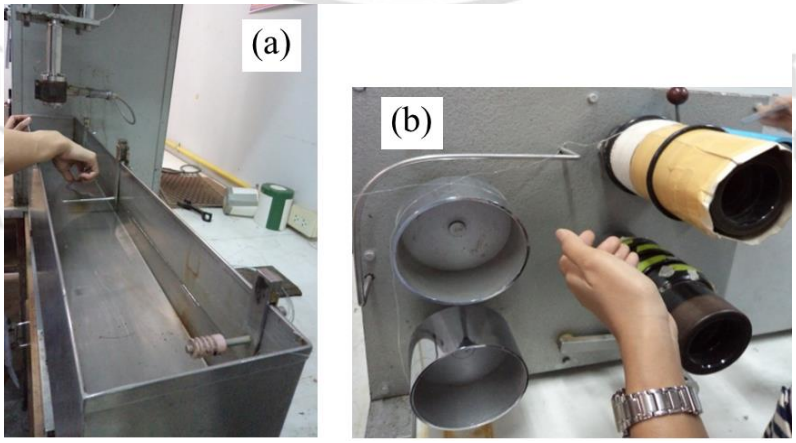

Figure 7.6 (a) Extruded filament being cooled (quenched) by passing through the cooling bath and (b) being wound around the take-up rollers before being collected on a bobbin.

Table 7.1 Processing conditions used for melt spinning of the PLC copolymers obtained using the solid tin(II) alkoxide initiators.

Initiator	Temp. (Rod) (^{o}C)	PLC Rod	Temp. (Spin) (^{o}C)	PLC Fibre	Fibre Properties
0.02 mol % $Sn(PEG300)_2$	120		135		Rough surface, brittle
0.01 mol % $Sn(PPG400)_2$	136		151		Rough surface, brittle
0.02 mol % $Sn(PPG400)_2$	134		149	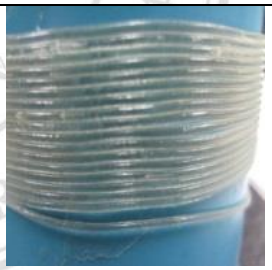	Smooth surface, flexible

Table 7.2 Processing conditions used for melt spinning of the PLC copolymers obtained using the liquid tin(II) alkoxide initiators.

Initiator	Temp. (Rod) (^oC)	PLC Rod	Temp. (Spin) (^oC)	PLC Fibre	Fibre Properties
0.01 mol % $Sn(Oct)_2$	136		152		Smooth surface, some voids, flexible
0.02 mol % $Sn(Oct)_2$	126		141		Smooth surface, some voids, flexible
0.01 mol % $[Sn(Oct)]_2DEG$ (2.1:1.0)	138		153		Smooth surface, homogeneous, flexible
0.02 mol % $[Sn(Oct)]_2DEG$ (2.1:1.0)	139		154		Smooth surface, homogeneous, less flexible

Table 7.2 (continued)

Initiator	Temp. (Rod) (^{o}C)	PLC Rod	Temp. (Spin) (^{o}C)	PLC Fibre	Fibre Properties
0.01 mol % $[Sn(Oct)]_2$DEG (3.0:1.0)	140		155		Smooth surface, homogeneous, flexible
0.02 mol % $[Sn(Oct)]_2$DEG (3.0:1.0)	131		146		Smooth surface, homogeneous, flexible
0.01 mol % $[Sn(Oct)]_2$EG	133		148		Smooth surface, homogeneous, hard
0.02 mol % $[Sn(Oct)]_2$EG	145		160		Smooth surface, homogeneous, hard

From the properties of the as-spun fibres obtained, only some of them were of sufficient strength that could be improved by off-line hot-drawing. Those which were able to be improved were those of the PLC copolymers synthesised using the 0.02 mol % $Sn(PPG400)_2$, 0.01 mol % $[Sn(Oct)]_2$DEG (2.1:1.0), 0.01 and 0.02 mol % $[Sn(Oct)]_2$DEG (3.0:1.0) initiators. The other as-spun fibres could not be hot-drawn because they were either too weak or too brittle (probably due to too low molecular weight) or contained internal voids.

7.3 Tensile Testing

The mechanical properties (tensile strength, % elongation at break, and Young's modulus) of the fibres at each stage of their processing were determined by tensile testing performed on a Lloyds LRX+ Universal Testing Machine, as illustrated previously in Figure 2.22. Fibre samples were cut into 35 cm lengths and their diameters measured accurately (± 0.001 mm) with a digital micrometer. Before testing, each fibre sample was left at fixed-length to equilibrate at the temperature and humidity of the instrument room. All tests were carried out with the fibre sample wound once around each of two bollard grips at 40 mm gauge length (Figure 2.23) and employing test conditions as described in section 2.5. The test results of the as-spun fibres are shown as stress-strain curves in Figure 7.7.

As shown in Figure 7.7, the as-spun fibres were very weak and highly extensible because their morphologies were largely unoriented. This was purpose-designed so that their mechanical properties could be improved off-line under controlled conditions. In this way, additional crystallinity and molecular orientation were gradually built into the as-spun fibres by a combination of off-line hot-drawing and annealing in order to give the required balance of mechanical properties (strength and flexibility) necessary for a monofilament surgical suture.

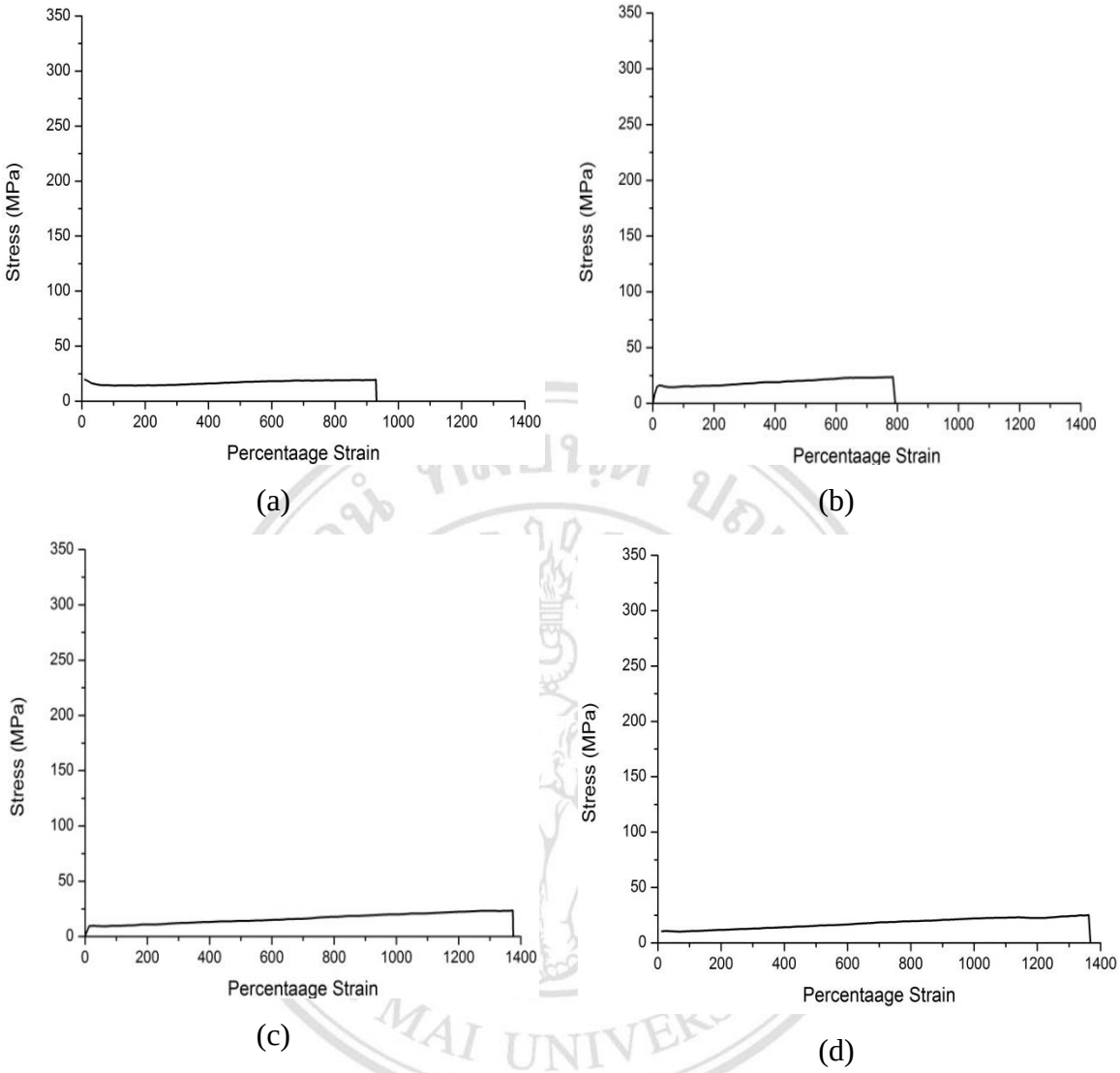

Figure 7.7 Stress-strain curves of the PLC as-spun fibres using initiators: (a) 0.02 mol % $Sn(PPG400)_2$, (b) 0.01 mol % $[Sn(Oct)]_2DEG$ (2.1:1), (c) 0.01 mol % $[Sn(Oct)]_2DEG$ (3.0:1) and (d) 0.02 mol % $[Sn(Oct)]_2DEG$ (3.0:1).

7.4 Off-line Hot-drawing and Annealing

Off-line hot-drawing of the as-spun fibres was carried out as a means of increasing the degree of chain orientation within the fibre, thereby strengthening the fibres in the direction of draw. Annealing was used to increase crystallinity and also provided an opportunity for molecular relaxation to occur by heating the fibre at a temperature intermediate between its T_g and T_m. In doing so, molecular motion is encouraged which can lead to chain segmental alignment and crystallisation, as described earlier in sections 2.4.2 and 2.4.3.

Hot-drawing at a temperature above the glass transition temperature (T_g) and around the crystallisation temperature (T_c) was employed in this project to enable greater extensibility and, as a result, higher orientation to strengthen the fibre. The degree of extension of the fibre may be represented by its draw ratio (λ) which is simply defined as:

$$\lambda = l / l_0$$

where l_0 and l are the initial and final lengths of the drawn fibre.

Determining a suitable draw rate and hot-draw temperature was essential for success. As high a draw rate as possible at each temperature was employed in order to enforce molecular alignment along the fibre axis, i.e. preferred directional orientation. Table 7.3 shows the conditions used in the off-line hot-drawing. The fibres processed under these various conditions were then tested with 3-5 test specimens being tested for each of the conditions used. The stress-strain curves for each condition are compared in Figures 7.8-7.11. The mechanical property test data derived from the curves are also summarized in Table 7.3. From the results, it was found that the fibre obtained from the PLC initiated by the 0.02 mol % $Sn(PPG400)_2$ solid initiator were too weak to be drawn. For the other fibres, the processing conditions listed in Table 7.3 were then used to determine the best conditions for mechanical property improvement.

After the 1st hot-drawing, the drawn fibre was annealed at fixed-length. Fixed annealing was necessary to allow molecular relaxation to occur so that a 2nd hot-drawing could be performed to as high a draw ratio as possible. Both the temperature and time of the intermediate annealing were adjusted to a fibre that was both strong and flexible enough to be drawn again. The conditions used in the off-line hot-drawing and annealing processes are shown in Table 7.4. Figures 7.12-7.14 show the stress-strain curves at each stage of processing including those of the corresponding as-spun fibres for comparison. The mechanical test results are summarized in Table 7.4.

7.5 Thermal Analysis by Differential Scanning Calorimetry

This methodology of off-line hot-drawing and annealing was facilitated by the fact that all of the PLC copolymers studied here were relatively slow-crystallizing materials which meant that their fibre morphology development could be controlled and followed more easily. The fibres after being processed at various conditions were characterised by DSC at the same heating rate of 10 ^{o}C/min under a dry nitrogen atmosphere. Their DSC thermograms are illustrated in Figures 7.15-7.17 and the results summarized in Table 7.4 for comparison. In the case of PLC, since the value of ΔH_m^* (heat of melting of a 100 % crystalline sample) is not known, ΔH_m-ΔH_c can be used instead to compare their relative crystallinities. Because PLC is a copolymer containing a distribution of copolymer compositions, the various temperature transitions (T_g, T_c, T_m) in the DSC curves tend to be rather broad compared with the respective homopolymers PL and PC. Despite this, the transitions in Figures 7.15-7.17 are clear enough for the associated thermal parameters to be determined reasonably accurately.

Table 7.3 Conditions used in the off-line hot-drawing of the PLC fibres and the resultant tensile properties.

Initiator System	**Processing Conditions**	**Draw Ratio (λ)**	**Tensile Properties**		
			Stress at Break (MPa)	**Strain at Break (%)**	**Initial Modulus * (MPa)**
0.02 mol % $Sn(PPG400)_2$	Hot-drawing 40 ^oC rate 540 % min^{-1}	3.2	99	155	382
	Hot-drawing 45 ^oC rate 900 % min^{-1}	4.8	107	152	311
0.01 mol % $[Sn(Oct)]_2DEG$ (2.1:1)	Hot-drawing 40 ^oC rate 520 % min^{-1}	5.1	146	83	622
	Hot-drawing 50 ^oC rate 1020 % min^{-1}	4.8	188	97	764
	Hot-drawing 60 ^oC rate 1150 % min^{-1}	5.4	163	75	700
0.01 mol % $[Sn(Oct)]_2DEG$ (3.0:1)	Hot-drawing 50 ^oC rate 520 % min^{-1}	4.8	132	142	536
	Hot-drawing 60 ^oC rate 1400 % min^{-1}	5.7	323	115	1086
	Hot-drawing 70 ^oC rate 550 % min^{-1}	6.1	52	59	330
0.02 mol % $[Sn(Oct)]_2DEG$ (3.0:1)	Hot-drawing 40 ^oC rate 490 % min^{-1}	5.1	134	237	357
	Hot-drawing 55 ^oC rate 1200 % min^{-1}	5.3	196	111	911
	Hot-drawing 70 ^oC rate 2740 % min^{-1}	5.7	236	119	656

* Estimated manually from the initial slop of the stress-strain curve

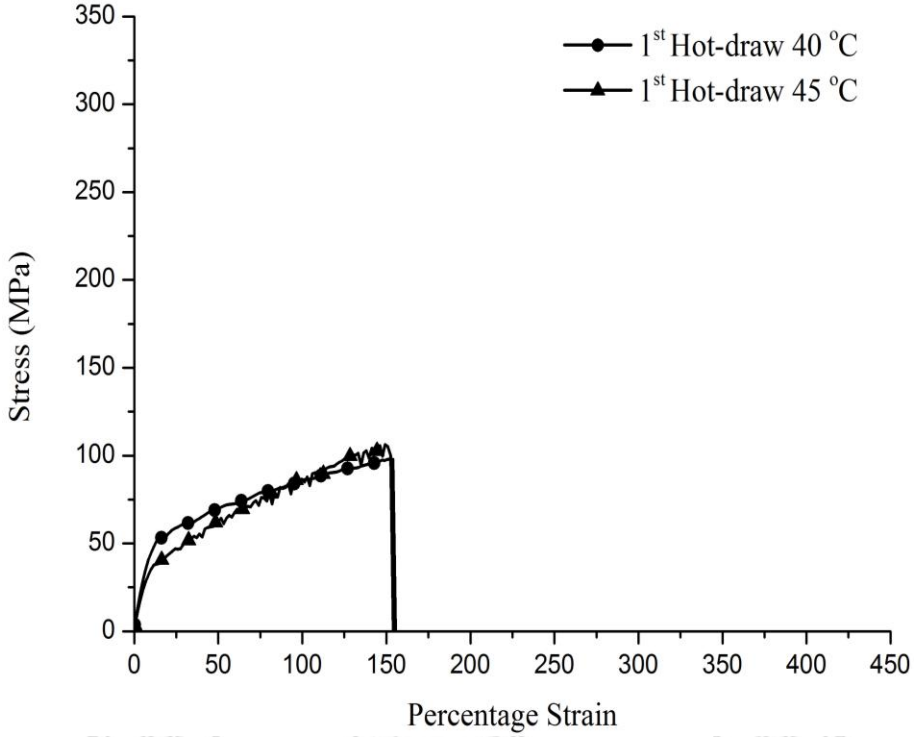

Figure 7.8 Stress-strain curves of the PLC fibres (0.02 mol % $Sn(PPG400)_2$ solid initiator) after 1st hot-drawing at 40 and 45 °C.

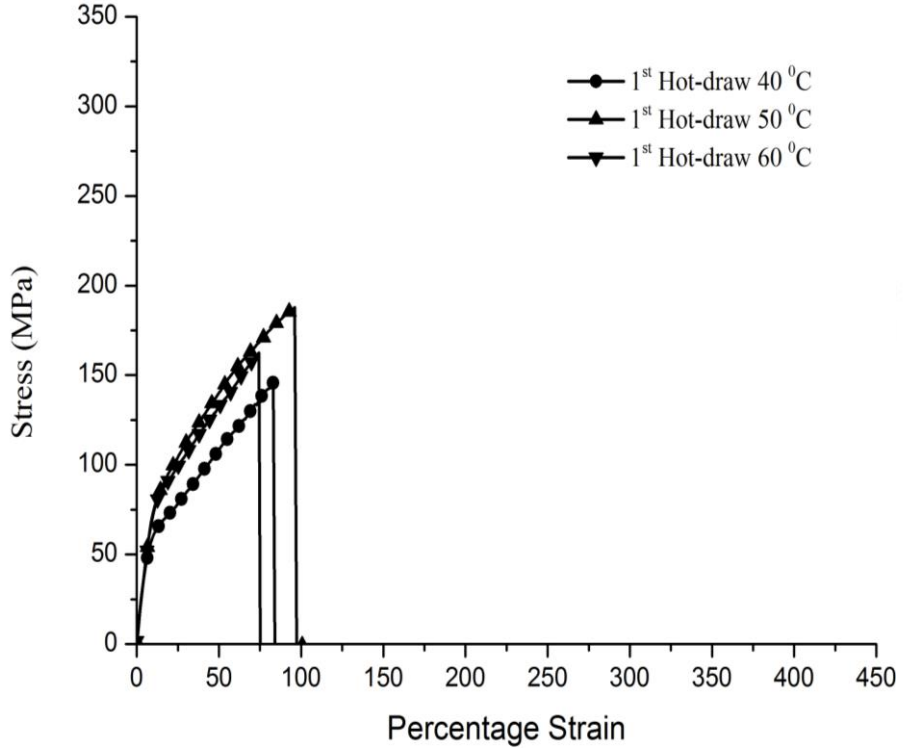

Figure 7.9 Stress-strain curves of the PLC fibres (0.01 mol % $[Sn(Oct)]_2$DEG (2.1:1) liquid initiator) after 1st hot-drawing at 40, 50 and 60 °C.

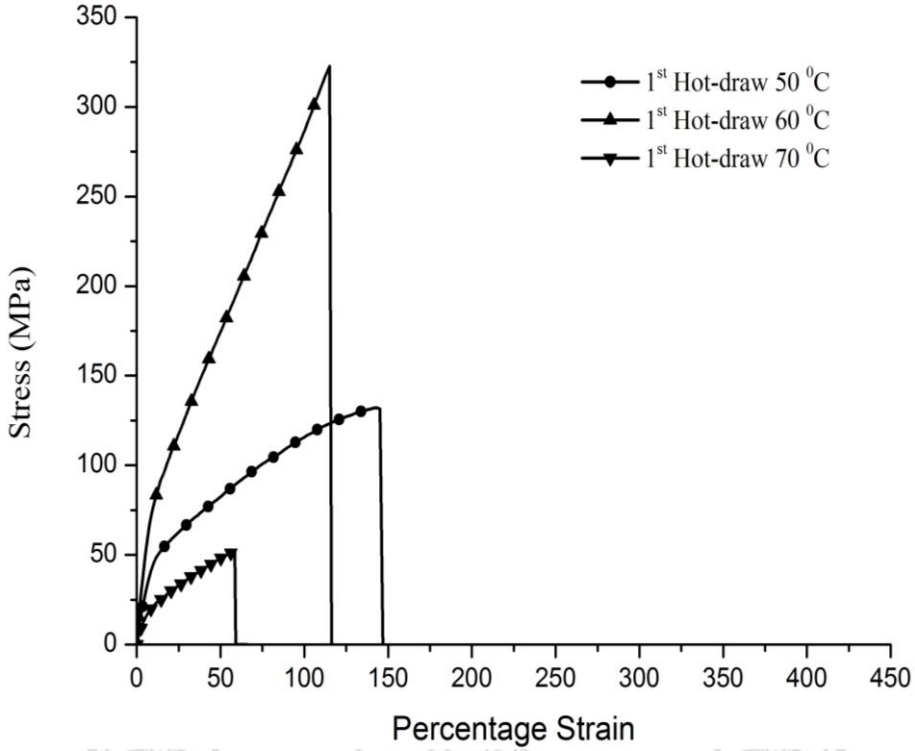

Figure 7.10 Stress-strain curves of the PLC fibres (0.01 mol % $[Sn(Oct)]_2$DEG (3.0:1) liquid initiator) after 1st hot-drawing at 50, 60 and 70 ^{o}C.

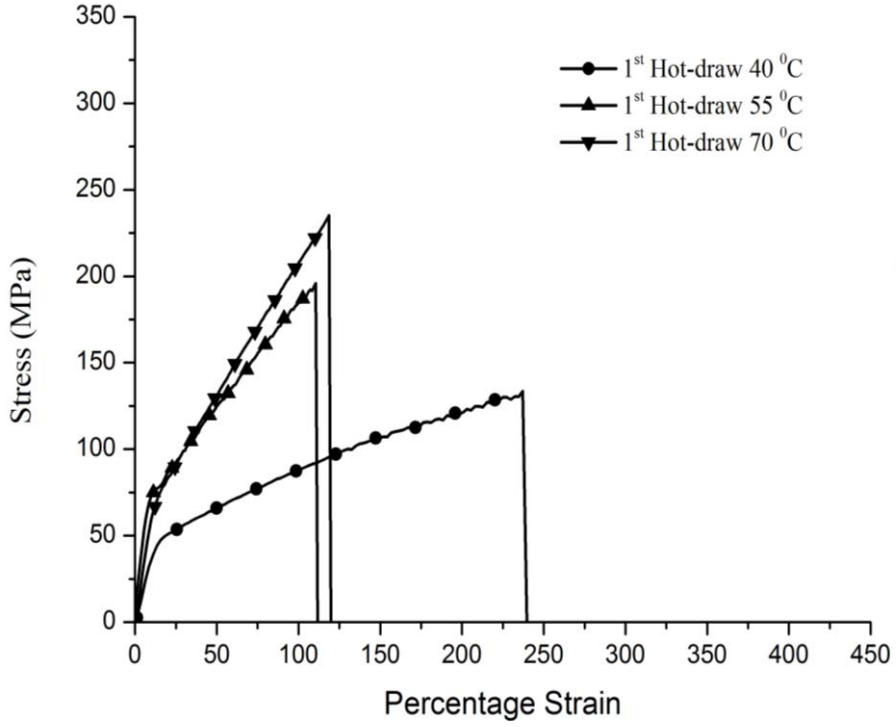

Figure 7.11 Stress-strain curves of the PLC fibres (0.02 mol % $[Sn(Oct)]_2$DEG (3.0:1) liquid initiator) after 1st hot-drawing at 40, 55 and 70 ^{o}C.

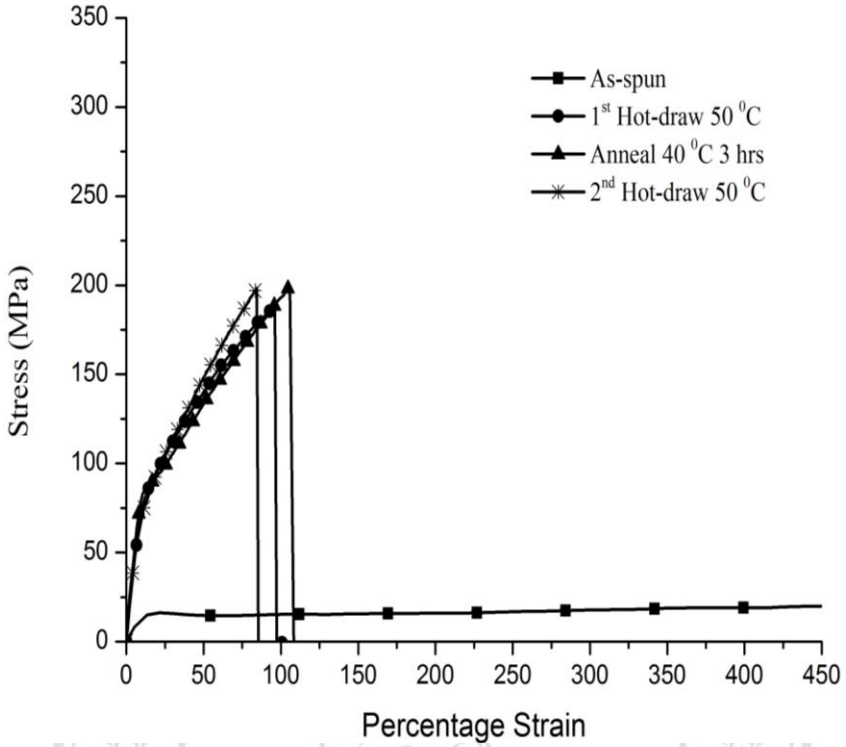

Figure 7.12 Stress-strain curves of the PLC fibres at various stages of processing. (0.01 mol % $[Sn(Oct)]_2$DEG (2.1:1) initiator)

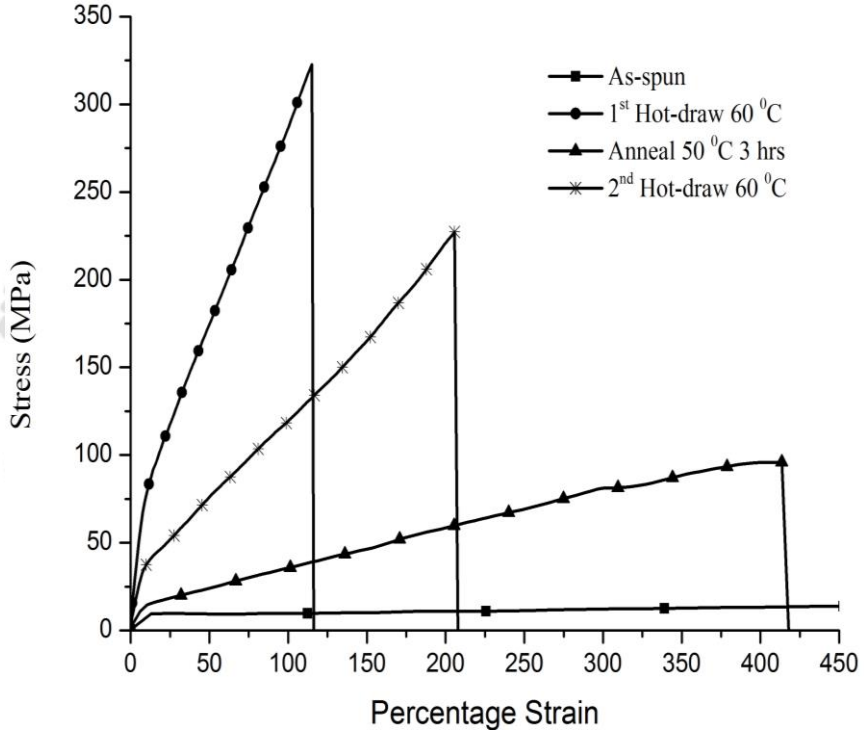

Figure 7.13 Stress-strain curve of the PLC fibres at various stages of processing. (0.01 mol % $[Sn(Oct)]_2$DEG (3:1) initiator)

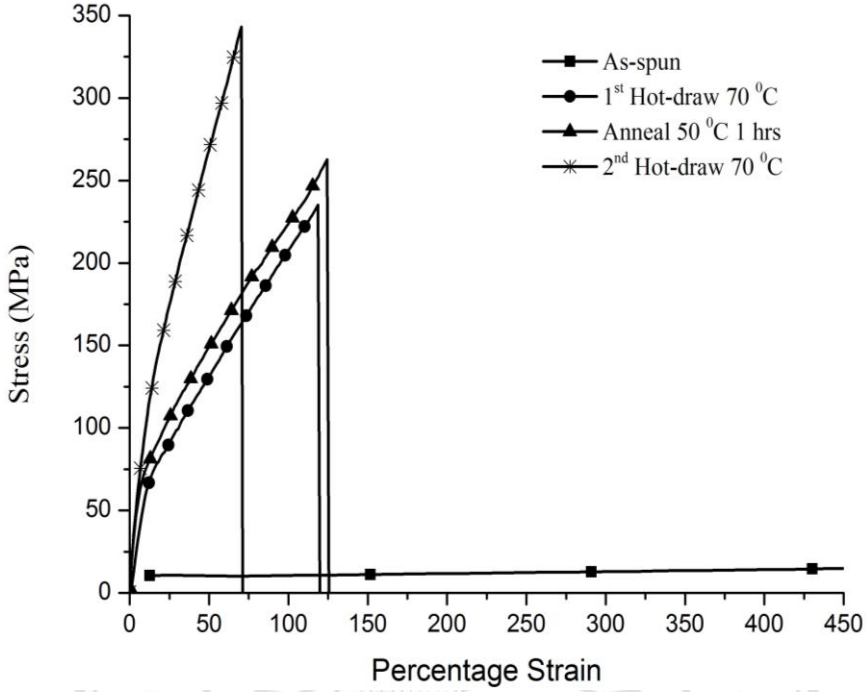

Figure 7.14 Stress-strain curves of the PLC fibres at various stages of processing. (0.02 mol % $[Sn(Oct)]_2$DEG (3:1) initiator)

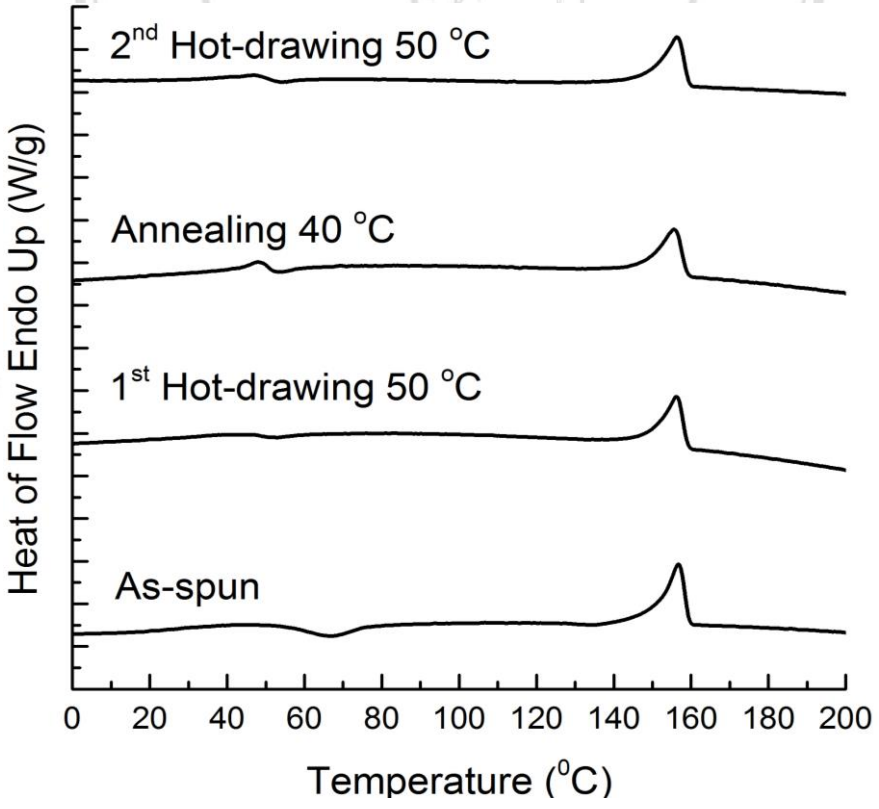

Figure 7.15 DSC thermograms of the PLC fibres at various stages of processing. (0.01 mol % $[Sn(Oct)]_2$DEG (2.1:1) initiator)

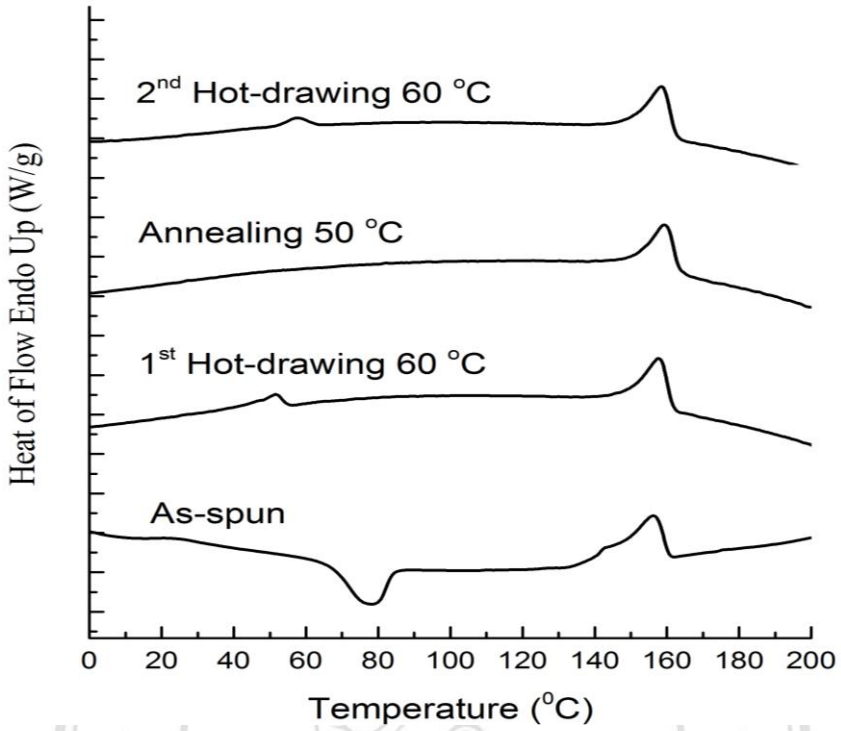

Figure 7.16 DSC thermograms of the PLC fibres at various stages of processing. (0.01 mol % $[Sn(Oct)]_2$DEG (3.0:1) initiator)

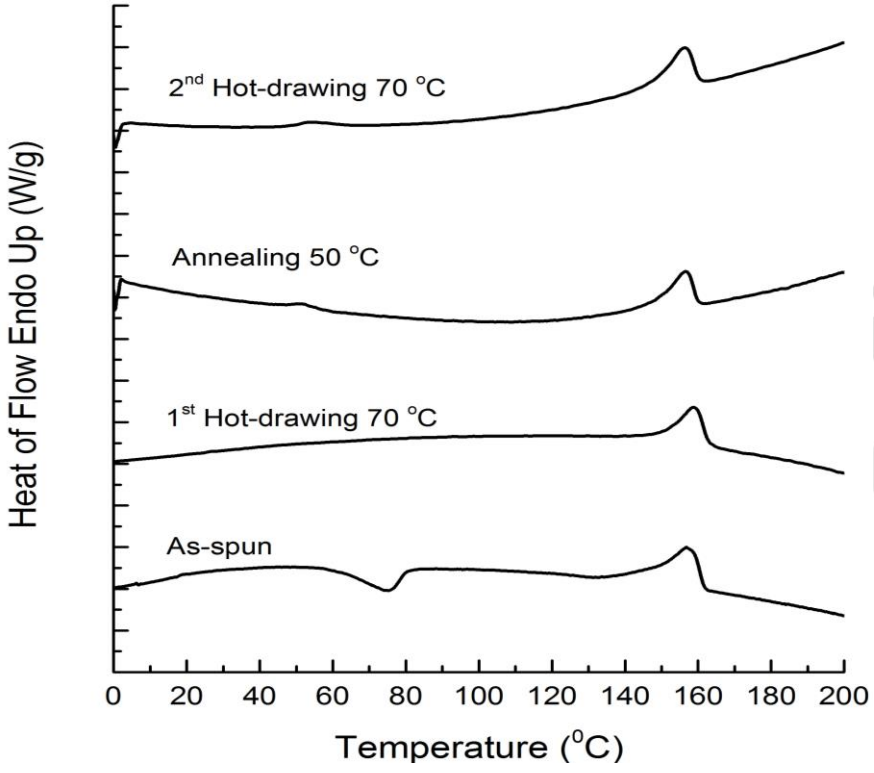

Figure 7.17 DSC thermograms of the PLC fibres at various stages of processing. (0.02 mol % $[Sn(Oct)]_2$DEG (3.0:1) initiator)

Table 7.4 Tensile test and DSC data for the PLC fibres at various stages of processing.

Initiator System	Processing Conditions	Draw Ratio (λ)	Tensile Testing			DSC					
			Stress at Break (MPa)	Strain at Break (%)	Initial Modulus * (MPa)	T_g (^oC)	T_c (^oC)	ΔH_c (J/g)	T_m (^oC)	ΔH_m (J/g)	ΔH_m-ΔH_c (J/g)
0.02 mol %	As-spun	-	20	931	240	24.5	88.5	21.0	148.5	23.3	2.3
$Sn(PPG400)_2$	Hot-drawing 40 ^oC	3.2	99	155	382	-	-	-	147.8	26.3	26.3
	Hot-drawing 45 ^oC	4.8	107	152	311	-	-	-	147.3	32.1	32.1
0.01mol %	As-spun	-	24	787	124	26.4	67.3	11.7	156.7	32.4	20.7
$[Sn(Oct)]_2$DEG (2.1:1)	Hot-drawing 50 ^oC	4.8	188	97	764	-	53.0	1.8	156.3	28.7	26.9
	Annealing 40 ^oC 3 hrs	4.8	201	107	764	-	53.3	1.8	155.7	28.8	27.0
	2^{nd} Hot-drawing 50 ^oC	6.9	199	85	700	-	54.0	1.1	156.3	29.3	27.3
0.01mol %	As-spun	-	24	1375	74	17.1	77.3	19.6	156..2	23.8	4.2
$[Sn(Oct)]_2$DEG (3.0:1)	Hot-drawing 60 ^oC	5.7	323	115	1086	-	-	-	157.5	22.6	22.6
	Annealing 50 ^oC 3 hrs	5.7	96	413	192	-	-	-	158.0	21.5	21.5
	2^{nd} Hot-drawing 60 ^oC	7.6	228	206	536	-	-	-	158.0	21.4	21.4
0.02 mol %	As-spun	-	25	1368	85	15.0	75.2	15.1	156.8	28.4	13.3
$[Sn(Oct)]_2$DEG (3.0:1)	Hot-drawing 70 ^oC	5.7	236	119	656	-	-	-	158.8	22.4	22.4
	Annealing 50 ^oC 1 hrs	5.7	264	125	1025	-	-	-	156.5	16.6	16.6
	2^{nd} Hot-drawing 70 ^oC	12.5	344	71	1367	-	-	-	156.3	19.5	19.5

* Estimated manually from the initial slop of the stress-strain curve

From the results shown in Figures 7.12-7.17 and combined in Table 7.4, the main conclusions that can be drawn are as follows:

1) The as-spun fibres were all very weak and highly extensible due to their low crystallinity and molecular orientation. This was purpose-designed so that the required oriented semi-crystalline morphology could be gradually built into the fibres in a series of controlled off-line hot-drawing and annealing steps.

2) Hot-drawing is a temperature-dependent process. The 1st hot-draw temperature which gave the highest strengths (stress at break) in Figures 7.8-7.11 were then used for subsequent annealing and 2nd hot-drawing. The main criterion for selecting a hot-draw temperature is that it must be above the fibre's T_g but not so high that the fibre becomes too soft. As seen in Figures 7.10 and 7.11 especially, changes in the hot-draw temperature, even within a relatively narrow temperature range, can have a marked effect on the strength of the fibre.

3) Hot-drawing is also a rate-dependent process. Furthermore, the rate and temperature of hot-drawing are interdependent. In this work, fast draw-rates were employed (Table 7.3) to a fixed length so that molecular alignment along the fibre axis could be enforced before relaxation could occur. Thus the rate as well as the temperature of hot-drawing had an important influence on the fibre's oriented morphology and both needed to be appropriate for each other.

4) Annealing at fixed length following the 1st hot-draw was carried out at a suitable temperature above T_g. The main purpose was to allow molecular relaxation to occur so that the fibre could be hot-drawn for a 2nd time in order to further increase molecular orientation and tensile strength. This sequence of processes produced a maximum tensile strength of 344 MPa (Figure 7.14) for the fibre obtained using the 0.02 mol % $[Sn(Oct)]_2$DEG (3.0:1) initiator.

5) From the results obtained, it can be concluded that the liquid initiator $[Sn(Oct)]_2$DEG gave the strongest fibres, possibly because the PLC obtained had higher molecular weights (see Table 6.2) which may have resulted in larger crystallites (higher T_m > 150 ^oC, see Figures 7.15-7.17). Importantly,

tensile strengths of higher than 300 MPa are comparable with those of commercial monofilament absorbable surgical sutures [117]. This shows the potential of those PLC fibres for further development as commercial materials.